# Lipid-Controlled Peptide Topology and Interactions in Bilayers: Structural Insights into the Synergistic Enhancement of the Antimicrobial Activities of PGLa and Magainin 2

Evgeniy S. Salnikov and Burkhard Bechinger*
Université de Strasbourg/Centre National de la Recherche Scientifique, Institut de Chimie, Strasbourg, France

ABSTRACT To gain further insight into the antimicrobial activities of cationic linear peptides, we investigated the topology of each of two peptides, PGLa and magainin 2, in oriented phospholipid bilayers in the presence and absence of the other peptide and as a function of the membrane lipid composition. Whereas proton-decoupled $^{15}N$ solid-state NMR spectroscopy indicates that magainin 2 exhibits stable in-plane alignments under all conditions investigated, PGLa adopts a number of different membrane topologies with considerable variations in tilt angle. Hydrophobic thickness is an important parameter that modulates the alignment of PGLa. In equimolar mixtures of PGLa and magainin 2, the former adopts transmembrane orientations in dimyristoyl-, but not 1-palmitoyl-2-oleoyl-, phospholipid bilayers, whereas magainin 2 remains associated with the surface in all cases. These results have important consequences for the mechanistic models explaining synergistic activities of the peptide mixtures and will be discussed. The ensemble of data suggests that the thinning of the dimyristoyl membranes caused by magainin 2 tips the topological equilibrium of PGLa toward a membrane-inserted configuration. Therefore, lipid-mediated interactions play a fundamental role in determining the topology of membrane peptides and proteins and thereby, possibly, in regulating their activities as well.

## INTRODUCTION

The increasing resistance of pathogens against the commonly used antibiotics is of major concern and requires urgent action and development of alternative treatments (1). Antimicrobial compounds are widespread in nature (2–4), and a promising approach is to search for bacteriocidal and fungicidal molecules to investigate their mechanism of action and use them as templates for the creation of more easy-to-prepare and/or more efficient analogs (5,6). In this manner, a large variety of host defense peptides have been discovered that are produced when infections occur and/or are stored in exposed tissues of animals and plants, thereby establishing a system that can react in a fast and efficient manner when infections arise (2–4). Cecropins and magainins were among the first peptides to be isolated, from insects and frogs, respectively (2,3). These cationic linear peptides exhibit a broad spectrum of antimicrobial activities, although the spectrum varies with sequence and the resulting differences in physicochemical properties. Several host defense peptides have also been shown to exhibit virucidal and tumoricidal activities (7,8).

The peptides of the magainin class carry an overall positive charge, and they exhibit pronounced interactions with phospholipid membranes, where they adopt amphipathic $\alpha$-helical conformations (9–11). By interacting with phospholipid bilayers, the peptides cause membrane pore formation, a decrease in Ohmic resistance, and a concomitant collapse of the TM electrochemical gradients by molecular mechanisms discussed below. Such modification of the membrane characteristics provides an explanation of the peptide cell-killing activities, as the formation of pores affects cellular respiration and deprives sensitive organisms of their source of energy (for reviews, see, e.g., Bechinger (5) and Shai (12)).

It is interesting to note that all-D-magainins, all-D-cecropins, cecropins with inverted sequences (retro), or inverse D-cecropins (retroenantio), all possess the high antibiotic and pore-forming activities of the parent L-enantiomer, which is taken as an indication that the cell-killing activities of these peptides are related to direct interactions with phospholipid membranes rather than through specific, chiral receptor interactions (13), although more recent evidence also points to the existence of intracellular targets once the bacterial or fungal membranes are crossed (for a review, see Brogden (14)).

When the lipid interactions of magainins and related cationic antimicrobial peptides were investigated by biophysical approaches, and in particular oriented solid-state NMR spectroscopy, the peptides were found to be preferentially aligned parallel to the membrane surface in a wide

*Submitted September 28, 2010, and accepted for publication January 31, 2011.*

*Correspondence: bechinger@unistra.fr

*Abbreviations used:* TM, transmembrane; CP, cross-polarization; di-C10:0-PC, 1,2-didecanoyl-*sn*-glycero-3-phosphocholine; di-C12:0-PC, 1,2-dilauroeyl-*sn*-glycero-3-phosphocholine; di-C20:1-PC, 1,2-dieicosenoyl-*sn*-glycero-3-phosphocholine; DMPC, 1,2-dimyristoyl-*sn*-glycero-3-phosphocholine; DMPG, 1,2-dimyristoyl-*sn*-glycero-3-phospho-(1′-*rac*-glycerol); IP, in-plane; NMR, nuclear magnetic resonance; POPC, 1-palmitoyl-2-oleoyl-*sn*-glycero-3-phosphocholine; POPE, 1-palmitoyl-2-oleoyl-*sn*-glycero-3-phosphoethanolamine; POPG, 1-palmitoyl-2-oleoyl-*sn*-glycero-3-phospho-(1′-*rac*-glycerol); RH, relative humidity; SUV, small unilamellar vesicles.

Editor: Marc Baldus.


0006-3495/11/03/1473/8 $2.00

doi: 10.1016/j.bpj.2011.01.070

variety of phospholipid bilayers (10,15–19), in excellent agreement with their amphipathic and highly charged character (5). IP alignments have also been observed for a number of magainin analogs (20–22). Based on such biophysical investigations, in combination with structure-activity studies (see, e.g., Vogt and Bechinger (23)), a number of models have been suggested to explain the pore-forming and antimicrobial properties of these cationic amphipathic peptides (for details, see Bechinger (5)). The models include formation of torroidal pores, where the peptides, together with the lipid, assemble into a supramolecular arrangement of high curvature (24,25). An alternative proposal is that the peptides accumulate at the membrane in an alignment parallel to the surface (12). Once this carpet becomes too dense, the membrane disintegrates and openings form. A third possibility is that at lower peptide concentrations, stochastic fluctuations of the IP peptides within the membrane surface account for the transient and stepwise increases in membrane conductivity observed in experiments (5). Finally, the amphipathic distribution of charges and hydrophobic residues was compared to the hydrophobic moment of detergents, which, depending on a number of parameters, such as lipid composition, peptide concentration, pH, and temperature, can exhibit a wide variety of different effects on lipid membranes, ranging from lysis to channel formation, or even an increase in the stability of lipid bilayers (26). Such models are confirmed by molecular modeling calculations showing that magainin 2 causes the formation of membrane lipidic pores without needing to adopt TM orientations or peptide-peptide contacts (27).

It has therefore been suggested that, in analogy to detergents, a full description of the peptide-lipid interactions requires extensive phase diagrams in which the previously suggested mechanisms, i.e., the carpet, wormhole, and lysis models, are represented by distinct areas (5,26). It should be noted that this knowledge has been used to successfully design short sequences as well as peptide mimetics with potent antimicrobial properties (28–32).

Even though these charged amphipathic sequences have been shown to associate with membranes in an IP fashion, more general models of membrane-associated peptides consider a series of equilibria where the peptides insert from the water phase to an interface-associated state, followed by membrane insertion and oligomerization (33,34). Such transitions between IP and TM alignments have been studied by solid-state NMR and oriented circular dichroism for a number of amphipathic sequences, and the membrane topology of these sequences has been analyzed as a function of hydration, peptide/lipid ratio, and lipid composition (35–37).

Another intriguing observation made with antimicrobial compounds is the synergistic enhancement of activities in naturally occurring cocktails of peptide antibiotics observed for combinations of magainin 2 and PGLa, as well as for other amphipathic peptides (11,38–41). In particular, when combinations of equimolar PGLa and magainin 2 in DMPC or DMPC/DMPG 3:1 (mole/mole) membranes were studied by $^{19}F$ or $^{2}H$ solid-state NMR spectroscopy, it was observed that PGLa adopts an alignment where the helix axis is oriented at ~22° relative to the membrane normal (42,43). These observations have been incorporated into a scenario where both peptides associate into a TM helical bundle, but at this time, the alignment of magainin 2 has to our knowledge not been tested experimentally.

Here, using $^{15}N$ solid-state NMR spectroscopy, we report, for the first time to our knowledge, the membrane alignment of magainin 2 in mixtures with PGLa as a function of lipid composition. The data thereby support models on how these (and possibly other) polypeptides interact within bilayer environments, and these models are conceptually different from previous propositions. To better understand the interactions that influence the bilayer topology of magainin and PGLa, additional $^{15}N$ solid-state NMR measurements in membranes of different lipid composition will be presented.

## MATERIALS AND METHODS

### Materials

The peptides PGLa and magainin 2 were prepared by solid-state synthesis using a Millipore 9050 automatic peptide synthesizer and Fmoc chemistry. Unlabeled PGLa was the generous gift of Michael Zasloff. The peptides (note sequences below) were prepared either unlabeled, where the isotopes occur in their natural abundance, or selectively labeled at the underlined positions using commercially available Fmoc-protected amino acid precursors (Euroistopes, Paris, France, or Promochem, Wesel, Germany). All lipids were from Avanti Polar Lipids (Alabaster, AL). The peptide sequences are

PGLa, GMASKAGAI<u>A</u> GKI<u>A</u>KVALKA L-NH2
Magainin 2, GIGKFLHSAK KFGK<u>A</u>FVGEI MNS

The underlined amino acid residues indicate where $^{15}N$ labeled amino acids (one at a time) have been incorporated. The peptides were purified by reverse-phase high-performance liquid chromatography, and their identity and purity were analyzed by analytical high-performance liquid chromatography and matrix-assisted laser desorption/ionization mass spectrometry (>90%).

### Sample preparation

A homogeneous mixture of lipid and peptide was obtained by codissolving the membrane components in chloroform/methanol (1:1 by volume). The solution was spread onto ultra thin coverglasses (8 × 22 mm, Marienfeld, Lauda-Königshofen, Germany) and dried, first in air and thereafter in high vacuum overnight. Membranes were equilibrated at 93% relative humidity, and where it was necessary to obtain hydration in the liquid-disordered state, the membranes were further exposed to higher temperatures (310 K) and 100% relative humidity for 2 h before the glass slides were stacked on top of each other.

### NMR spectroscopy

Proton-decoupled $^{31}P$ solid-state NMR spectra were acquired at 161.953 MHz on a Bruker (Rheinstetten, Germany) Avance widebore 400 NMR

spectrometer equipped with a double-resonance flat-coil probe (44). A phase-cycled Hahn-echo pulse sequence (45) with a $\pi/2$ pulse of 2.5 $\mu$s, a spectral width of 75 kHz, an echo delay of 40 $\mu$s, and a recycle delay of 3 s were used. Spectra were referenced externally to 85% $H_3PO_4$ at 0 ppm.

Proton-decoupled $^{15}$N cross-polarization (CP) spectra of static aligned samples were acquired at 40.54 MHz on a Bruker Avance widebore 400-MHz NMR spectrometer equipped with a double-resonance flat-coil probe (44). An adiabatic CP pulse sequence was used (46) with spectral width, acquisition time, CP contact time, and recycle delay time of 75 kHz, 3.5 ms, 0.8 ms, and 3 s, respectively. The $^1$H $\pi/2$ pulse and spinal 64 heteronuclear decoupling field strengths were 42 kHz. A total of 40,000 scans were accumulated, and the spectra were zero-filled to 4096 points. The spectra were recorded at temperatures well above the gel-to-liquid phase transitions of the lipids (e.g., $T_c = 271$ K and 296 K for POPC and DMPC, respectively (for other lipids, cf. Table 2 of Harzer and Bechinger (47)). Typically, a 200-Hz exponential line-broadening was applied before Fourier transformation. Spectra were externally referenced to $^{15}NH_4Cl$ at 40.0 ppm. An Oxford temperature control unit was used.

## RESULTS AND DISCUSSION

In a first series of experiments, mixtures of PGLa and magainin were reconstituted into oriented DMPC/DMPG 3:1 (mole/mole) membranes, and the topological state of each of the cationic peptides was analyzed by circular dichroism and proton-decoupled $^{15}$N solid-state NMR spectroscopy. In the presence of phosphatidylcholine small unilamellar vesicles (SUVs), the circular dicihroism spectra of the peptides, alone or when present in equimolar amounts, indicate that the peptides retain their predominantly helical conformation even in a mixture ((39) and the Supporting Material). Furthermore, although the different curvature of SUVs may cause subtle conformational alterations when compared to planar lipid bilayers, the data are in good agreement with the presence of helical secondary structures throughout major parts of the sequences, as has been previously observed in a wide variety of membrane environments (9,10,16). For solid-state NMR spectroscopy, the peptides were mixed in such a manner that either one only (Fig. 1, *A* and *C*) or both (Fig. 1 *B*) carried a $^{15}$N label within their helical domain (9,10). Due to the unique properties of the $^{15}$N amide chemical-shift tensor, the approximate alignment of helical peptides can be obtained directly from the $^{15}$N chemical shift measured from such samples (48). Whereas TM helical alignments are characterized by $^{15}$N chemical shifts in the 200-ppm region, peptides that orient along the membrane surface exhibit values of $<$100 ppm.

The proton-decoupled $^{15}$N spectrum of [$^{15}$N-Ala$^{14}$]-PGLa in the presence of unlabeled magainin 2 (Fig. 1 *A*) shows that it exhibits a predominant $^{15}$N signal intensity at 178 ppm, indicating that in the presence of magainin 2, [$^{15}$N-Ala$^{14}$]-PGLa adopts tilt angles that agree with TM alignments, as observed in previous investigations using $^2$H and $^{19}$F solid-state NMR spectroscopy (42,49). However, when magainin 2 was labeled with $^{15}$N and investigated in the presence of an equimolar amount of unlabeled PGLa, the chemical shift at 82 ppm indicates that [$^{15}$N-Ala$^{15}$]-magainin 2 remains aligned parallel to the surface in the presence (Fig. 1 *C*) or absence of the other peptide (15,16,50). The data are confirmed by a third sample, where both peptides are simultaneously labeled with $^{15}$N (Fig. 1 *B*).

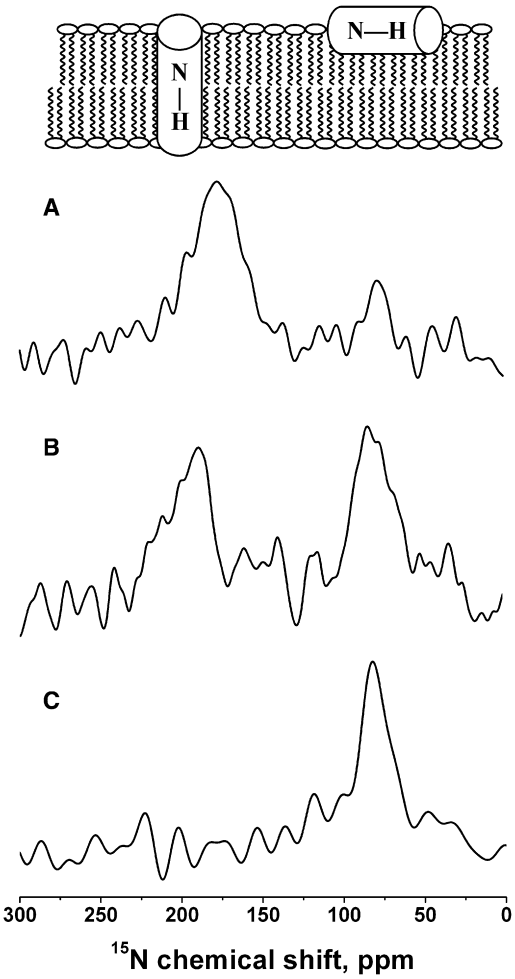


FIGURE 1 Proton-decoupled $^{15}$N solid-state NMR spectra of peptide mixtures reconstituted into oriented DMPC/DMPG 3:1 (mole/mole) membranes at 310 K. Samples were equilibrated at 93% RH in all cases. (*A*) [$^{15}$N-Ala$^{14}$]-PGLa and unlabeled magainin 2. (*B*) [$^{15}$N-Ala$^{14}$]-PGLa and [$^{15}$N-Ala$^{15}$]-magainin 2. (*C*) Unlabeled PGLa and [$^{15}$N-Ala$^{15}$]-magainin 2. In all cases, the molar ratios of PGLa/magainin 2/DMPC/DMPG were 1:1:75:25. The bilayer model above the NMR spectra illustrates the correlation between the $^{15}$N chemical shift and the membrane alignment of helical peptides. The spectrum shown in *A* is characterized by a predominant TM and a smaller IP signal intensity, indicating that a sensitive equilibrium is governing the PGLa membrane interactions (cf. text for details).

In a next step, the effect of lipid composition on the membrane topology of PGLa and magainin 2 was further investigated. It should be noted that most of the early measurements on these cationic antimicrobial peptides were performed after they had been individually reconstituted into 1-palmitoyl-2-oleoyl-phospholipid bilayers, and these investigations always indicated that the peptides align parallel to the membrane surface (10,15,16,50–52). Therefore, to test whether the TM alignment of PGLa (Fig. 1, *A*

and *B*) (42,49) is solely due to the presence of magainin or is also related to the DMPC/DMPG lipid composition, additional samples were prepared in which mixtures of PGLa and magainin2 were reconstituted into POPC or POPC/POPG 3:1 (mole/mole) membranes (Fig. 2). The $^{15}$N chemical shifts for [$^{15}$N-Ala$^{14}$]-PGLa (Fig. 2, *A* and *C*) and [$^{15}$N-Ala$^{15}$]-magainin 2 (Fig. 2, *B* and *D*) of 89 and 84 ppm, respectively, indicate that in all four membranes tested, both peptides adopt IP alignments. It should be mentioned that differences in the magainin 2 interactions with DMPC and POPC membranes have also been noted in previous biophysical investigations (24,53). Thus, in the model bilayers believed to best represent the 1-saturated-2-unsaturated fatty acyl composition and the hydrophobic thickness of natural membranes, both peptides consistently exhibit IP orientations in the presence (Fig. 2) or absence of the interaction partner (10,15,16,50–52).

Most mechanistic studies of the synergy between magainin 2 and PGLa have been performed on lipid membranes of fatty acyl composition closely related to those used during the experiments shown in Fig. 2 (39,54,55). The pioneering biophysical work by Matsuzaki and co-workers shows that the membrane pores formed by PGLa, magainin 2, or mixtures of the two peptides follow similar mechanisms, which are characterized by lipid flip-flop and peptide translocation. The kinetics of these two processes parallel that of pore formation, as evidenced by calcein release from preformed vesicles (39). Those authors suggested that synergy

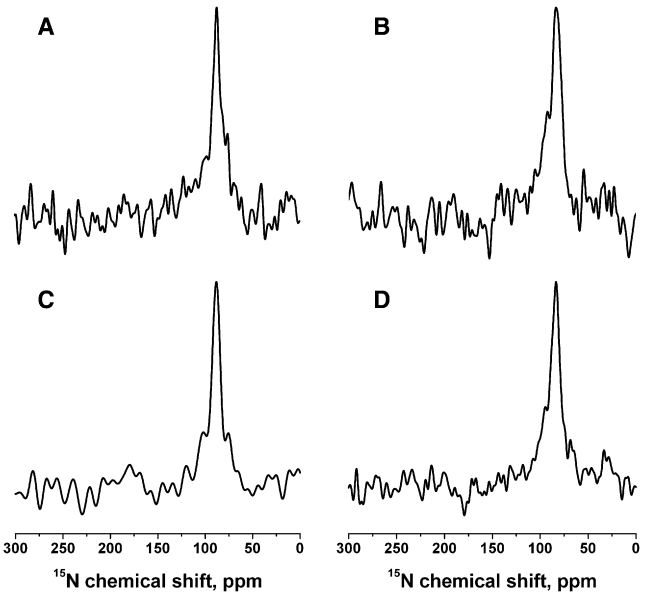


FIGURE 2 Proton-decoupled $^{15}$N solid-state NMR spectra of peptide mixtures reconstituted into oriented POPC/POPG 3:1 (mole/mole) (*A* and *B*) or POPC (*C* and *D*) membranes at 310 K. (*A* and *C*) [$^{15}$N-Ala$^{14}$]-PGLa and unlabeled magainin 2. (*B* and *D*) Unlabeled PGLa and [$^{15}$N-Ala$^{15}$]-magainin 2. The molar ratios of PGLa/magainin 2/POPC/POPG were 1:1:75:25 and those of PGLa/magainin 2/POPC were 1:1:100. Samples were equilibrated at 93% RH in all cases.

arises from the combination of the faster formation of membrane openings due to the presence of PGLa with a pore lifetime intermediate to those measured for magainin or PGLa alone (39). Mutagenesis experiments and the study of covalently linked dimers suggest that magainin 2 and PGLa transiently form a heterodimer of parallel helices (54,55), which, according to this work, reside on the surface of the membranes when investigated in palmitoyl-oleoyl phospholipid bilayers (Fig. 2).

Another question arises as to how the TM insertion of PGLa in dimyristoyl phospholipids can be explained, when at the same time, the data shown in Figs. 1 and 2 indicate that the peptides in combination do not form a heteromeric TM channel structure (42,49). An alternative model proposes that the peptides influence each other by modulating the membrane properties (cf. Fig. 3 *C* in Bechinger (5)), similar to suggestions made to explain the regulation of biological activity of larger membrane proteins (56). It should be noted that membrane hydrophobic thickness has previously been shown to have a pronounced influence on the membrane topology of other amphipathic peptides, such as peptaibols or model sequences (47,57–59). Therefore, we speculated that the well-known membrane-thinning effect of magainin 2 (60) could have a significant effect also on PGLa topology.

To test this hypothesis, we investigated the alignment of [$^{15}$N-Ala$^{14}$]-PGLa alone in phosphatidylcholine membranes of different fatty acyl chain composition. Indeed, when reconstituted into phosphatidylcholine bilayers, the [$^{15}$N-Ala$^{14}$]-PGLa helix changes from an IP orientation in di-C20:1-PC bilayers ($^{15}$N chemical shift 87 ppm) (Fig. 3 *A*), POPC (Fig. 3 *B*), POPE/POPG 3:1 (mole/mole), or POPC/POPG 3:1 (mole/mole) (10,50) to smaller tilt angles (i.e., deviating from a perfect IP orientation) in the presence of the thinner DMPC/DMPG 3:1 (mole/mole) ($^{15}$N chemical shift (108 $\pm$ 23) ppm (Fig. 3 *C*)) and di-C12:0-PC bilayers (155 ppm, Fig. 3 *D*). Finally, the $^{15}$N chemical shift of [$^{15}$N-Ala$^{14}$]-PGLa in di-C10:0-PC exhibits a broad chemical shift distribution between 105 and 160 ppm (maximum at 132 ppm), suggesting that in thin membranes, the tilt angle of the membrane-spanning peptide increases again, as has been observed previously for TM model peptides (47), or when the membrane alignments of alamethicin in DMPC and POPC are compared to each other (58). Fig. 4 provides a graphical summary of the $^{15}$N chemical shifts measured and the corresponding PGLa topologies, as well as a definition of the tilt angle, $\theta$. In contrast, magainin 2 exhibits an IP alignment even when associated with the di-C10:0-PC membrane (the $^{15}$N chemical shift of position 15 is 85 ppm (Fig. 3 *E*)), as well as under all conditions investigated previously (10,15,16,50–52). Note that the proton-decoupled $^{31}$P NMR spectra of all samples are indicative of well-aligned phospholipid bilayers (Fig. 3, *G–L*).

Thus, the data show that the hydrophobic thickness of the membrane has a pronounced influence on the PGLa

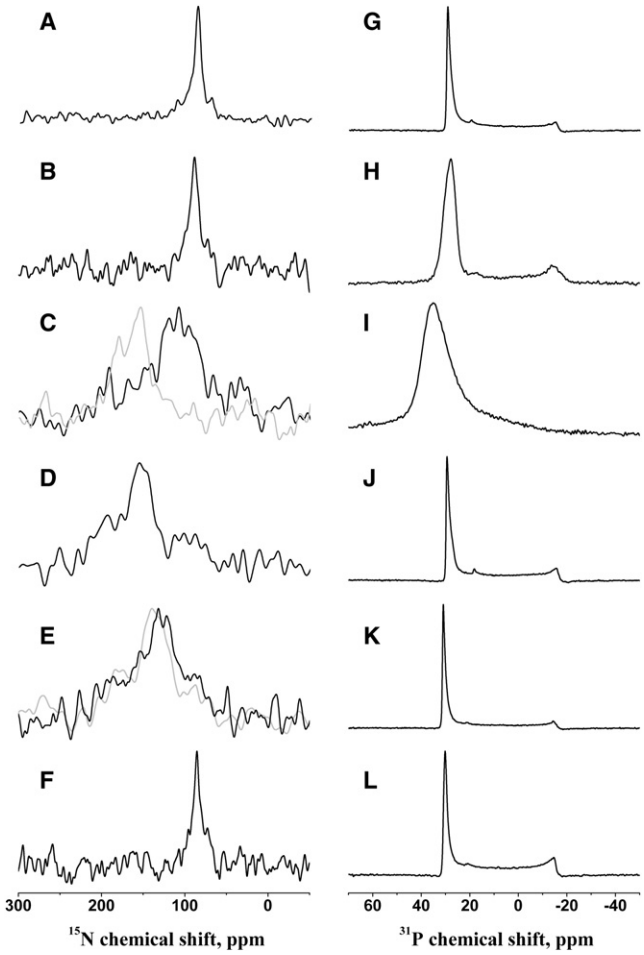


FIGURE 3 (*A–F*) Proton-decoupled $^{15}$N solid-state NMR spectra of [$^{15}$N-Ala$^{14}$]-PGLa (*A–E*) or [$^{15}$N-Ala$^{15}$]-magainin 2 (*F*) in aligned membranes of different lipid compositions. (*G–L*) Proton-decoupled $^{31}$P solid-state NMR spectra of the samples in *A–F*. Lipid compositions were di-C20:1-PC, 295 K (*A* and *G*); POPC, 310 K (*B* and *H*); DMPC/DMPG 3:1 (mole/mole), 310 K; di-C12:0-PC, 295 K (*C–J*); PGLa in di-C10:0-PC, 295 K (*E* and *K*) (for comparison, the spectrum obtained from [$^{15}$N-Ala$^{10}$]-PGLa is shown in gray in *E*); and magainin 2 in di-C10:0-PC, 295 K (*F* and *L*). Peptide concentrations were 2 mol % in all cases. Samples were equilibrated at 93% RH, except in the case of the gray spectrum in *C*, which was equilibrated at 100% RH before data acquisition.

topology, but not on that of magainin 2, and we suspect that this difference is due to the larger hydrophobic angle of the PGLa helix (39) concomitant with the smaller number of polar residues being transferred from the interface into the membrane interior upon peptide reorientation. Whereas the fatty acyl chain length controls the PGLa topology, few or no orientational effects are observed due to the presence of negatively charged phospholipids either for this peptide (42,49) (Fig. 3, *B* and *C*) or for the magainin 2 helix (15).

The series of investigations shown in Figs. 2 and 3 are indicative that in addition to the IP, tilted, and TM alignments, which have been described previously (42,49) and which correspond to $^{15}$N chemical shifts for [$^{15}$N-Ala$^{14}$]-PGLa of ~85 ppm (Figs. 1 *C* and 3, *A* and *B*; $\theta = 81°$ according to Strandberg et al. (49)), 108 ppm (Fig. 3 *C*, *black line*; $\theta = 53°$), and 180 ppm (Fig. 1 *A*; $\theta = 22°$), additional intermediates are observed (Fig. 3, *D* and *E*, 155 and 132 ppm, respectively). Note that next to the spectral maxima can be seen shoulders ranging into the 155- and 180-ppm regions (Figs. 3, *C–E*), suggesting that in the case of the thinner membranes, the dominant topologies are in exchange with other, less tilted alignments. The resulting spectral line broadening degrades the signal/noise ratio of some of the spectra, although the integrated signal intensity of all spectra shown agrees well with the number of accumulations. The TM alignment was confirmed by the $^{15}$N chemical shift spectrum of [$^{15}$N-Ala$^{10}$]-PGLa in di-C10:0-PC (Fig. 3 *E*, *gray line*), thereby indicating that the structural and topological preferences extend over the central core region of the peptide.

It is notable that the less tilted alignment, although also present by the 180 ppm shoulder in the spectra shown in Fig. 3, *C–E*, is most stable in the presence of magainin 2 (Fig. 1, *A* and *B*), suggesting that the physical properties of the membrane in the presence of magainin 2 and/or the interactions between the peptides stabilize this topology. Such peptide-peptide interactions could involve long-range electrostatic interactions and/or more specific molecular recognition (39,61). Whereas the strong electrostatic repulsion between the cationic peptides seems to destabilize close molecular interactions, the experimental evidence seems to favor a well-defined structural arrangement. First, in the presence of magainin 2, the equilibrium of PGLa alignments shown in Fig. 4 is shifted toward a configuration exhibiting a $^{15}$N chemical shift of ~180 ppm (Fig. 1, *A* and *B*, and 4 *B*), and very similar $^{15}$N chemical shifts of PGLa/magainin mixtures are observed when the $^{15}$N solid-state NMR spectra obtained from oriented di-C10:0-PC (not shown) and DMPC/DMPG bilayers (Fig. 1) are compared to each other. Furthermore, a recent structure of a PGLa-magainin 2 heterodimer in the presence of dodecylphosphocholine micelles exhibits a number of interresidual contacts and almost perpendicular relative alignments of the two peptides, although it is not obvious how to place this structure into an intact lipid bilayer, as the hydrophobic faces of both helices are exposed to the outside of the dimer (11).

Assuming a constant rotational pitch angle the $^{15}$N chemical-shift range covering 85–180 ppm corresponds to changes of the helical tilt of ~45°, an angular range that considerably increases when additional movements around the helix axis occur (47,48). It is of interest that the $^{15}$N chemical shifts indicate that even in its TM state, the peptide remains significantly tilted regardless of the hydrophobic thickness of the membrane, and one may speculate that this topology assures a better positioning of the K5 and K19 side chains for snorkeling to the membrane surface (62) and/or for PGLa-PGLa interactions (63).

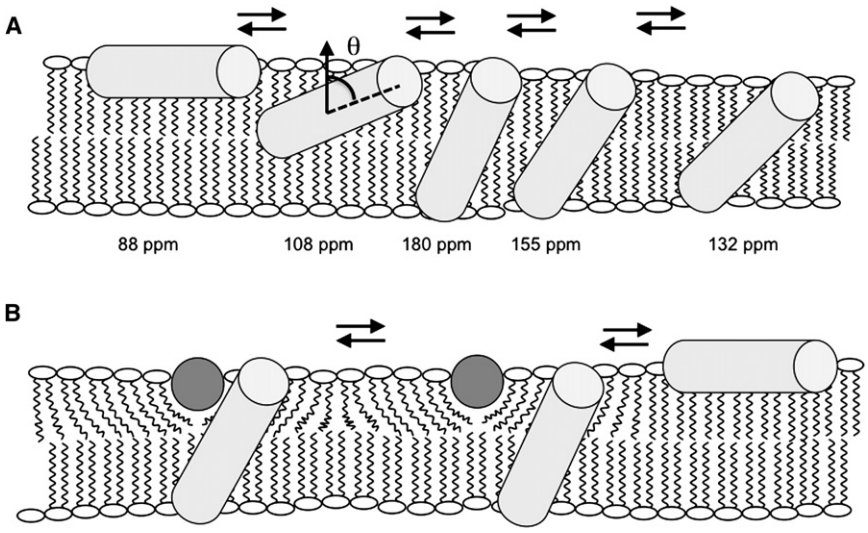


FIGURE 4 Models of PGLa and magainin 2 helix alignments in oriented lipid bilayers. The PGLa helices are sketched as light gray cylinders, and the magainin 2 helices are viewed along their long axis and shown as dark gray circles. (*A*) Sketch of how PGLa alone adjusts its alignment to the membrane hydrophobic thickness. Whereas the peptide orients along the membrane surface in thick PC membranes, it spans bilayers made of shorter fatty acyl chains. The approximate $^{15}$N chemical shifts of [$^{15}$N-Ala$^{14}$]-PGLa are also indicated, as is the definition of the tilt angle, $\theta$, between the membrane normal and the helix long axis. (*B*) Illustration of how membrane thinning caused by magainin 2 can trigger topological alterations of PGLa in DMPC (but not POPC) membranes (cf. text for details). Small populations or transient additional intermediates (as shown in *A*) may exist also for PGLa in the presence of magainin 2 but they have been omitted for clarity.

It has been observed that several amphipathic peptides, including PGLa, can adopt a number of topological states depending on lipid composition, peptide/lipid ratio, hydration, temperature, pH, and the presence of additional membrane components (19,36,64,65), a situation that is also illustrated in Fig. 4 *A*. From a thermodynamic perspective, these transitions have been characterized by equilibria such as $\mathrm{IP} \Leftrightarrow \mathrm{titled}_1 \Leftrightarrow \mathrm{titled}_2 \Leftrightarrow \mathrm{titled}_3 \Leftrightarrow .... \Leftrightarrow \mathrm{TM}_1 \Leftrightarrow \mathrm{TM}_2 \Leftrightarrow \mathrm{TM}_3 \Leftrightarrow \mathrm{etc}$.

The different TM states could represent, for example, different tilt angles and/or oligomerization states, and the possibility exists that the IP topology is also to be diversified into additional substates. When directly comparing the ensemble of IP and TM states, interaction energies contributing to the corresponding Gibbs free energy of transition, $\Delta G_{\mathrm{IP} \Leftrightarrow \mathrm{TM}}$, arise, for example, from changes of hydrophobic contributions when amino acid side chains move from the interface to the membrane interior (34,66), contributions from the peptide-induced packing defects of the phospholipid membrane, hydrophobic mismatch, and peptide-peptide interactions (36,47).

The hydrophobic-mismatch contribution has been found to be particularly important in investigations of peptaibols, such as the 15-residue peptides zervamicin II or ampullosporin A (57,58), similar to the behavior of PGLa observed here (Fig. 3, *A–E*). Although the previous studies indicated that hydrophobic mismatch has a pronounced influence on peptide topology, it was also found that the peptaibols adopt TM alignments only within bilayers that are thinner than one would expect from their hydrophobic length alone. Therefore, to explain such differences, other interactions need to be taken into consideration as well.

In the case of PGLa, a TM alignment is observed when the thickness of the bilayer is reduced to di-C12:0-phosphatidylcholine, which in its pure form exhibits a hydrophobic thickness of 19.5 Å (68). This span finds its geometric correspondence in an $\alpha$-helix encompassing 13 amino acids, although the number of residues exposed to the hydrophobic regions of the membrane may be slightly different due to changes in the secondary structure of the peptide and/or adaptations of the fatty acyl chain order parameter that occur under conditions of hydrophobic mismatch (47,69). In particular, the PGLa sequence A6–L18 is of corresponding dimensions. It encompasses two cationic residues and is flanked by two additional lysines whose side chains potentially snorkel to the surface (see primary sequences of the peptides in the Methods section). Indeed, previous solid-state NMR and molecular modeling investigations showed that two (but not three) lysines can be accommodated with TM alignments of amphiphilic model peptides, as long as other interactions provide suitable driving forces for compensation (64). These considerations offer an explanation for the stable IP alignment of magainin 2, where three lysines accumulate in the central region of the peptide, when at the same time PGLa exhibits a more flexible topology.

To further test the effect of hydrophobic mismatch on the PGLa topology, the hydration level of the sample shown in Fig. 3 *C* was increased through equilibration at 100% rather than 93% RH. Augmentation of the water content in the bilayer interface has previously been shown to increase the lateral headgroup spacing and thereby results in a decrease of the hydrophobic thickness of phosphatidylcholine membranes (60). Indeed, the $^{15}$N chemical shift spectrum of [$^{15}$N-Ala$^{14}$]-PGLa in DMPC/DMPG 3:1 (mole/mole) at full hydration (Fig. 3 *C*, *gray line*) closely corresponds to that obtained after equilibrating the di-C12:0-PC sample at 93% RH (Fig. 3 *D*). In contrast, the PGLa alignment remains in a stable IP alignment even after the hydration of the POPC/POPG sample is augmented (not shown).

In conclusion, the data presented indicate that the membrane hydrophobic thickness is an important parameter that modulates the PGLa but not the magainin 2 topology. It has been shown that addition of magainin 2 to DMPC membranes results in a decrease of the bilayer thickness by a few Ångstroms (60). It is interesting to note that in equimolar mixtures of PGLa and magainin 2, the former adopts TM orientations in liquid-disordered dimyristoyl membranes but not in the thicker palmitoyl-oleoyl phospholipid bilayers (70). The ensemble of data suggests that the thinning of the dimyristoyl membranes caused by magainin 2 sufficiently tips the topological equilibria of PGLa toward a membrane inserted configuration (Fig. 4 *B*). However, both peptides, alone or in combination, remain surface-associated in palmitoyl-oleoyl-phospholipid membranes, suggesting that this IP topology forms the structural basis for the synergistic enhancements of antimicrobial and channel-forming activities.

## SUPPORTING MATERIAL

A figure showing CD spectra of magainin 2, PGLa, and their mixture is available at http://www.biophysj.org/biophysj/supplemental/S0006-3495S0006-3495(11)00200-1.

We are most grateful to Mike Zasloff for the kind gift of unlabelled PGLa and to Erick Goormaghtigh for attenuated total reflectance Fourier transform infrared measurement of oriented membranes confirming the tilt angles of PGLa in POPC and in thin membranes. The financial contributions of the Agence National de la Recherche and Vaincre la Mucoviscidose are acknowledged.

## REFERENCES

1. Novak, R., B. Henriques, …, E. Tuomanen. 1999. Emergence of vancomycin tolerance in *Streptococcus pneumoniae*. *Nature.* 399:590–593.
2. Zasloff, M. 2002. Antimicrobial peptides in health and disease. *N. Engl. J. Med.* 347:1199–1200.
3. Boman, H. G. 2003. Antibacterial peptides: basic facts and emerging concepts. *J. Intern. Med.* 254:197–215.
4. García-Olmedo, F., A. Molina, …, P. Rodríguez-Palenzuéla. 1998. Plant defense peptides. *Biopolymers.* 47:479–491.
5. Bechinger, B. 1999. The structure, dynamics and orientation of antimicrobial peptides in membranes by solid-state NMR spectroscopy. *Biochim. Biophys. Acta.* 1462:157–183.
6. Hwang, P. M., and H. J. Vogel. 1998. Structure-function relationships of antimicrobial peptides. *Biochem. Cell Biol.* 76:235–246.
7. Cruciani, R. A., J. L. Barker, …, O. Colamonici. 1991. Antibiotic magainins exert cytolytic activity against transformed cell lines through channel formation. *Proc. Natl. Acad. Sci. USA.* 88:3792–3796.
8. Chen, H. M., W. Wang, …, S. C. Chan. 1997. Effects of the antibacterial peptide cecropin B and its analogs, cecropins B1 and B2, on liposomes, bacteria and cancer cells. *Biochim. Biophys. Acta.* 1336:171–179.
9. Gesell, J., M. Zasloff, and S. J. Opella. 1997. Two-dimensional 1H NMR experiments show that the 23-residue magainin antibiotic peptide is an $\alpha$-helix in dodecylphosphocholine micelles, sodium dodecylsulfate micelles, and trifluoroethanol/water solution. *J. Biomol. NMR.* 9:127–135.
10. Bechinger, B., M. Zasloff, and S. J. Opella. 1998. Structure and dynamics of the antibiotic peptide PGLa in membranes by multidimensional solution and solid-state nuclear magnetic resonance spectroscopy. *Biophys. J.* 74:981–987.
11. Haney, E. F., H. N. Hunter, …, H. J. Vogel. 2009. Solution NMR studies of amphibian antimicrobial peptides: linking structure to function? *Biochim. Biophys. Acta.* 1788:1639–1655.
12. Shai, Y. 1999. Mechanism of the binding, insertion and destabilization of phospholipid bilayer membranes by $\alpha$-helical antimicrobial and cell nonselective membrane-lytic peptides. *Biochim. Biophys. Acta.* 1462:55–70.
13. Wade, D., A. Boman, …, R. B. Merrifield. 1990. All-D amino acid-containing channel-forming antibiotic peptides. *Proc. Natl. Acad. Sci. USA.* 87:4761–4765.
14. Brogden, K. A. 2005. Antimicrobial peptides: pore formers or metabolic inhibitors in bacteria? *Nat. Rev. Microbiol.* 3:238–250.
15. Bechinger, B., M. Zasloff, and S. J. Opella. 1992. Structure and interactions of magainin antibiotic peptides in lipid bilayers: a solid-state nuclear magnetic resonance investigation. *Biophys. J.* 62:12–14.
16. Bechinger, B., M. Zasloff, and S. J. Opella. 1993. Structure and orientation of the antibiotic peptide magainin in membranes by solid-state nuclear magnetic resonance spectroscopy. *Protein Sci.* 2:2077–2084.
17. Pouny, Y., D. Rapaport, …, Y. Shai. 1992. Interaction of antimicrobial dermaseptin and its fluorescently labeled analogues with phospholipid membranes. *Biochemistry.* 31:12416–12423.
18. Matsuzaki, K., O. Murase, …, K. Miyajima. 1994. Orientational and aggregational states of magainin 2 in phospholipid bilayers. *Biochemistry.* 33:3342–3349.
19. Tremouilhac, P., E. Strandberg, …, A. S. Ulrich. 2006. Conditions affecting the re-alignment of the antimicrobial peptide PGLa in membranes as monitored by solid state 2H-NMR. *Biochim. Biophys. Acta.* 1758:1330–1342.
20. Ramamoorthy, A., S. Thennarasu, …, L. Maloy. 2006. Solid-state NMR investigation of the membrane-disrupting mechanism of antimicrobial peptides MSI-78 and MSI-594 derived from magainin 2 and melittin. *Biophys. J.* 91:206–216.
21. Strandberg, E., N. Kanithasen, …, A. S. Ulrich. 2008. Solid-state NMR analysis comparing the designer-made antibiotic MSI-103 with its parent peptide PGLa in lipid bilayers. *Biochemistry.* 47:2601–2616.
22. Mason, A. J., W. Moussaoui, …, B. Bechinger. 2009. Structural determinants of antimicrobial and antiplasmodial activity and selectivity in histidine-rich amphipathic cationic peptides. *J. Biol. Chem.* 284:119–133.
23. Vogt, T. C. B., and B. Bechinger. 1999. The interactions of histidine-containing amphipathic helical peptide antibiotics with lipid bilayers. The effects of charges and pH. *J. Biol. Chem.* 274:29115–29121.
24. Ludtke, S. J., K. He, …, H. W. Huang. 1996. Membrane pores induced by magainin. *Biochemistry.* 35:13723–13728.
25. Matsuzaki, K. 1998. Magainins as paradigm for the mode of action of pore forming polypeptides. *Biochim. Biophys. Acta.* 1376:391–400.
26. Bechinger, B. 2009. Rationalizing the membrane interactions of cationic amphipathic antimicrobial peptides by their molecular shape. *Curr. Opin. Colloid Interf. Sci.* 14:349–355.
27. Leontiadou, H., A. E. Mark, and S. J. Marrink. 2006. Antimicrobial peptides in action. *J. Am. Chem. Soc.* 128:12156–12161.
28. Makovitzki, A., J. Baram, and Y. Shai. 2008. Antimicrobial lipopolypeptides composed of palmitoyl di- and tricationic peptides: in vitro and in vivo activities, self-assembly to nanostructures, and a plausible mode of action. *Biochemistry.* 47:10630–10636.
29. Patch, J. A., and A. E. Barron. 2003. Helical peptoid mimics of magainin-2 amide. *J. Am. Chem. Soc.* 125:12092–12093.
30. Porter, E. A., B. Weisblum, and S. H. Gellman. 2002. Mimicry of host-defense peptides by unnatural oligomers: antimicrobial $\beta$-peptides. *J. Am. Chem. Soc.* 124:7324–7330.
31. Kuroda, K., and W. F. DeGrado. 2005. Amphiphilic polymethacrylate derivatives as antimicrobial agents. *J. Am. Chem. Soc.* 127:4128–4129.

32. Violette, A., S. Fournel, …, G. Guichard. 2006. Mimicking helical antibacterial peptides with nonpeptidic folding oligomers. *Chem. Biol.* 13:531–538.
33. Sansom, M. S. P. 1991. The biophysics of peptide models of ion channels. *Prog. Biophys. Mol. Biol.* 55:139–235.
34. White, S. H., and W. C. Wimley. 1999. Membrane protein folding and stability: physical principles. *Annu. Rev. Biophys. Biomol. Struct.* 28:319–365.
35. Huang, H. W., and Y. Wu. 1991. Lipid-alamethicin interactions influence alamethicin orientation. *Biophys. J.* 60:1079–1087.
36. Bechinger, B. 1996. Towards membrane protein design: pH-sensitive topology of histidine-containing polypeptides. *J. Mol. Biol.* 263: 768–775.
37. Huang, H. W. 2006. Molecular mechanism of antimicrobial peptides: the origin of cooperativity. *Biochim. Biophys. Acta.* 1758:1292–1302.
38. Westerhoff, H. V., M. Zasloff, …, D. Juretić. 1995. Functional synergism of the magainins PGLa and magainin-2 in *Escherichia coli*, tumor cells and liposomes. *Eur. J. Biochem.* 228:257–264.
39. Matsuzaki, K., Y. Mitani, …, K. Miyajima. 1998. Mechanism of synergism between antimicrobial peptides magainin 2 and PGLa. *Biochemistry.* 37:15144–15153.
40. Bashford, C. L., G. M. Alder, …, C. A. Pasternak. 1986. Membrane damage by hemolytic viruses, toxins, complement, and other cytotoxic agents. A common mechanism blocked by divalent cations. *J. Biol. Chem.* 261:9300–9308.
41. Liu, S. P., L. Zhou, …, R. W. Beuerman. 2010. Multivalent antimicrobial peptides as therapeutics: design principles and structural diversities. *Int. J. Pept. Res. Ther.* 16:199–213.
42. Tremouilhac, P., E. Strandberg, …, A. S. Ulrich. 2006. Synergistic transmembrane alignment of the antimicrobial heterodimer PGLa/magainin. *J. Biol. Chem.* 281:32089–32094.
43. Strandberg, E., S. Esteban-Martín, …, A. S. Ulrich. 2009. Orientation and dynamics of peptides in membranes calculated from 2H-NMR data. *Biophys. J.* 96:3223–3232.
44. Bechinger, B., and S. J. Opella. 1991. Flat-coil probe for NMR spectroscopy of oriented membrane samples. *J. Magn. Reson.* 95:585–588.
45. Rance, M., and R. A. Byrd. 1983. Obtaining high-fidelity spin-1/2 powder spectra in anisotropic media: phase-cycled Hahn echo spectroscopy. *J. Magn. Reson.* 52:221–240.
46. Hediger, S., B. H. Meier, and R. R. Ernst. 1995. Adiabatic passage Hartmann-Hahn cross polarization in NMR under magic angle sample spinning. *Chem. Phys. Lett.* 240:449–456.
47. Harzer, U., and B. Bechinger. 2000. Alignment of lysine-anchored membrane peptides under conditions of hydrophobic mismatch: a CD, $^{15}$N and $^{31}$P solid-state NMR spectroscopy investigation. *Biochemistry.* 39:13106–13114.
48. Bechinger, B., and C. Sizun. 2003. Alignment and structural analysis of membrane polypeptides by $^{15}$N and $^{31}$P solid-state NMR spectroscopy. *Concepts Magn. Reson.* 18A:130–145.
49. Strandberg, E., P. Tremouilhac, …, A. S. Ulrich. 2009. Synergistic transmembrane insertion of the heterodimeric PGLa/magainin 2 complex studied by solid-state NMR. *Biochim. Biophys. Acta.* 1788:1667–1679.
50. Bechinger, B., L. M. Gierasch, …, S. J. Opella. 1996. Orientations of helical peptides in membrane bilayers by solid state NMR spectroscopy. *Solid State Nucl. Magn. Reson.* 7:185–191.
51. Bechinger, B., Y. Kim, …, S. J. Opella. 1991. Orientations of amphipathic helical peptides in membrane bilayers determined by solid-state NMR spectroscopy. *J. Biomol. NMR.* 1:167–173.
52. Ramamoorthy, A., F. M. Marassi, …, S. J. Opella. 1995. Three-dimensional solid-state NMR spectroscopy of a peptide oriented in membrane bilayers. *J. Biomol. NMR.* 6:329–334.
53. Bechinger, B. 2005. Detergent-like properties of magainin antibiotic peptides: a $^{31}$P solid-state NMR spectroscopy study. *Biochim. Biophys. Acta.* 1712:101–108.
54. Hara, T., Y. Mitani, …, K. Matsuzaki. 2001. Heterodimer formation between the antimicrobial peptides magainin 2 and PGLa in lipid bilayers: a cross-linking study. *Biochemistry.* 40:12395–12399.
55. Nishida, M., Y. Imura, …, K. Matsuzaki. 2007. Interaction of a magainin-PGLa hybrid peptide with membranes: insight into the mechanism of synergism. *Biochemistry.* 46:14284–14290.
56. Shearman, G. C., G. S. Attard, …, R. H. Templer. 2007. Using membrane stress to our advantage. *Biochem. Soc. Trans.* 35:498–501.
57. Bechinger, B., D. A. Skladnev, …, J. Raap. 2001. $^{15}$N and $^{31}$P solid-state NMR investigations on the orientation of zervamicin II and alamethicin in phosphatidylcholine membranes. *Biochemistry.* 40:9428–9437.
58. Salnikov, E. S., H. Friedrich, …, B. Bechinger. 2009. Structure and alignment of the membrane-associated peptaibols ampullosporin A and alamethicin by oriented $^{15}$N and $^{31}$P solid-state NMR spectroscopy. *Biophys. J.* 96:86–100.
59. Strandberg, E., S. Ozdirekcan, …, J. A. Killian. 2004. Tilt angles of transmembrane model peptides in oriented and non-oriented lipid bilayers as determined by $^{2}$H solid-state NMR. *Biophys. J.* 86:3709–3721.
60. Ludtke, S., K. He, and H. Huang. 1995. Membrane thinning caused by magainin 2. *Biochemistry.* 34:16764–16769.
61. Cruciani, R. A., J. L. Barker, …, E. F. Stanley. 1992. Magainin 2, a natural antibiotic from frog skin, forms ion channels in lipid bilayer membranes. *Eur. J. Pharmacol.* 226:287–296.
62. Monné, M., I. Nilsson, …, G. von Heijne. 1998. Positively and negatively charged residues have different effects on the position in the membrane of a model transmembrane helix. *J. Mol. Biol.* 284:1177–1183.
63. Glaser, R. W., C. Sachse, …, A. S. Ulrich. 2005. Concentration-dependent realignment of the antimicrobial peptide PGLa in lipid membranes observed by solid-state 19F-NMR. *Biophys. J.* 88:3392–3397.
64. Vogt, T. C. B., P. Ducarme, …, B. Bechinger. 2000. The topology of lysine-containing amphipathic peptides in bilayers by circular dichroism, solid-state NMR and molecular modelling. *Biophys. J.* 79:2644–2656.
65. Huang, H. W. 2000. Action of antimicrobial peptides: two-state model. *Biochemistry.* 39:8347–8352.
66. Aisenbrey, C., E. Goormaghtigh, …, B. Bechinger. 2006. Translocation of amino acyl residues from the membrane interface to the hydrophobic core: thermodynamic model and experimental analysis using ATR-FTIR spectroscopy. *Mol. Membr. Biol.* 23:363–374.
67. Reference deleted in proof.
68. Lewis, B. A., and D. M. Engelman. 1983. Lipid bilayer thickness varies linearly with acyl chain length in fluid phosphatidylcholine vesicles. *J. Mol. Biol.* 166:211–217.
69. Killian, J. A. 1998. Hydrophobic mismatch between proteins and lipids in membranes. *Biochim. Biophys. Acta.* 1376:401–415.
70. Kucerka, N., S. Tristram-Nagle, and J. F. Nagle. 2005. Structure of fully hydrated fluid phase lipid bilayers with monounsaturated chains. *J. Membr. Biol.* 208:193–202.